NIH Public Access
Author Manuscript
Microcirculation. Author manuscript; available in PMC 2012 April 24.

Published in final edited form as:
Microcirculation. 2009 November ; 16(8): 667–684. doi:10.3109/10739680903133722.

IMPACT OF CHRONIC ANTI-CHOLESTEROL THERAPY ON DEVELOPMENT OF MICROVASCULAR RAREFACTION IN THE METABOLIC SYNDROME

Adam G. Goodwill[1,2], **Stephanie J. Frisbee**[1,3], **Phoebe A. Stapleton**[1,4], **Milinda E. James**[1,2], and **Jefferson C. Frisbee**[1,2]

[1]Center for Cardiovascular and Respiratory Sciences West Virginia University School of Medicine, Morgantown, WV 26506

[2]Department of Physiology and Pharmacology, West Virginia University School of Medicine, Morgantown, WV 26506

[3]Department of Community Medicine, West Virginia University School of Medicine, Morgantown, WV 26506

[4]Department of Exercise Physiology West Virginia University School of Medicine, Morgantown, WV 26506

Abstract

Object—The obese Zucker rat (OZR) model of the metabolic syndrome is partly characterized by moderate hypercholesterolemia in addition to other contributing co-morbidities. Previous results suggest that vascular dysfunction in OZR is associated with chronic reduction in vascular nitric oxide (NO) bioavailability and chronic inflammation, both frequently associated with hypercholesterolemia. As such, we evaluated the impact of chronic cholesterol reducing therapy on the development of impaired skeletal muscle arteriolar reactivity and microvessel density in OZR and its impact on chronic inflammation and NO bioavailability.

Materials and Methods—Beginning at 7 weeks of age, male OZR were treated with gemfibrozil, probucol, atorvastatin or simvastatin (in chow) for 10 weeks. Subsequently, plasma and vascular samples were collected for biochemical/molecular analyses, while arteriolar reactivity and microvessel network structure were assessed using established methodologies after 3, 6 and 10 weeks of drug therapy

Results—All interventions were equally effective at reducing total cholesterol, although only the statins also blunted the progressive reductions to vascular NO bioavailability, evidenced by greater maintenance of acetylcholine-induced dilator responses, an attenuation of adrenergic constrictor reactivity, and an improvement in agonist-induced NO production. Comparably, while minimal improvements to arteriolar wall mechanics were identified with any of the interventions, chronic statin treatment reduced the rate of microvessel rarefaction in OZR. Associated with these improvements was a striking statin-induced reduction in inflammation in OZR, such that numerous markers of inflammation were correlated with improved microvascular reactivity and density. However, using multivariate discriminant analyses, plasma RANTES, IL-10, MCP-1 and TNF-α were determined to be the strongest contributors to differences between groups, although their relative importance varied with time.

Send Correspondence to: Jefferson C. Frisbee, Ph.D. Center for Cardiovascular and Respiratory Sciences Department of Physiology and Pharmacology Robert C. Byrd Health Sciences Center PO Box 9105 West Virginia University School of Medicine Morgantown, WV 26505 Phone: (304) 293-6527 Fax: (304) 293-5513 jfrisbee@hsc.wvu.edu.

NIH-PA Author Manuscript
NIH-PA Author Manuscript
NIH-PA Author Manuscript

NIH-PA Author Manuscript

NIH-PA Author Manuscript

NIH-PA Author Manuscript

Conclusions—While the positive impact of chronic statin treatment on vascular outcomes in the metabolic syndrome are independent of changes to total cholesterol, and are more strongly associated with improvements to vascular NO bioavailability and attenuated inflammation, these results provide both a spatial and temporal framework for targeted investigation into mechanistic determinants of vasculopathy in the metabolic syndrome.

Keywords

regulation of skeletal muscle perfusion; vascular remodeling; vascular reactivity; rodent models of obesity; nitric oxide bioavailability; chronic inflammation

INTRODUCTION

Arising from a chronic hyperphagia which originates due to non-functional leptin receptor gene and an impaired satiety reflex (5,23), the obese Zucker rat (OZR) rapidly develops insulin resistance, hypertriglyceridemia and a moderate hypertension (43). Combined with the parallel creation of a pro-thrombotic, pro-oxidant and pro-inflammatory environment, OZR are considered to be an excellent model for the clinical condition termed the metabolic syndrome (47). Associated with these systemic pathologies, we and others have defined numerous impairments to microvascular structure and function in OZR which negatively impact skeletal muscle perfusion, both under resting conditions (15,18,19), in response to elevated metabolic demand (18,19,50,51), following recovery from vascular occlusion (15) and during hemorrhage (16). Chronic treatment of the metabolic syndrome with exercise (13,52) or of individual contributing elements through pharmacological intervention (10,16,17,48) have resulted in improvements to microvascular outcomes, as well as to perfusion responses within skeletal muscle (13,52), and have implicated potential mechanisms through which these improvements may be manifested. Recently, results from our laboratory have suggested that the chronic reduction in vascular nitric oxide (NO) bioavailability that accompanies development of the metabolic syndrome in OZR is well correlated with the severity of the reduction in skeletal muscle microvessel density (16). Ongoing studies have also suggested that while this microvascular rarefaction is hypertension-independent (17), exercise-based interventions that not only increase vascular NO bioavailability, but also blunt the severity of the chronic inflammatory state in OZR, may be an excellent predictor of the ability to prevent microvessel loss within the periphery (13).

Within the metabolic syndrome in OZR is an elevation in plasma cholesterol levels that, while consistent, is more moderate as compared to the profound elevations determined for plasma triglycerides. Given the severity of many indices of vascular dysfunction in OZR, the extent to which elevated plasma cholesterol contributes to these impairments in currently unclear. However, treatment of hypercholesterolemia with 3-hydroxy-3-methylglutaryl coenzyme A (HMG Co-A) reductase inhibitors (“statins”) has not only the well-documented impact of lowering circulating plasma LDL and total cholesterol levels (21,35), but also has been identified as having the beneficial impacts of increasing vascular NO bioavailability (3,34) and blunting plasma markers of chronic inflammation (11,32,35). Notably, it has been suggested that improvements to vascular function in human subjects or animals afflicted with hypercholesterolemia may reflect these pleiotropic effects of statin therapy rather than the direct impact of anti-cholesterol therapy itself (3,26,31). However, the extent to which these reflect independent ameliorative effects or effects which are strongly correlated remains unclear.

The purpose of the present study was to determine the impact of chronic anti-cholesterol therapy on the temporal development of impairments to microvascular reactivity and

NIH-PA Author Manuscript

NIH-PA Author Manuscript

NIH-PA Author Manuscript

network structure in skeletal muscle of OZR manifesting the metabolic syndrome. Further, the present study also attempted to demonstrate differences in treatment effectiveness of more recently developed statin medications as compared to traditional anti-cholesterol medications that do not fall into this category. The tested hypothesis was that chronic ingestion of anti-cholesterol therapies would better maintain microvascular structure and function in OZR, although the benefit of these effects would be due to improvements in vascular NO bioavailability and chronic inflammation, rather than effects on plasma cholesterol *per se*.

MATERIALS AND METHODS

Animals

Male lean (LZR) and OZR (Harlan) fed standard chow and drinking water (see below) *ad libitum* were housed at the West Virginia University Health Sciences Center and all protocols received prior IACUC approval. At 6–7 weeks of age, LZR and OZR were divided into five groups within each strain:

1. control (maintained on normal chow)
2. treatment with gemfibrozil [GEM; maintained on chow containing 50 mg/kg/d gemfibrozil, a fibric acid derivative and PPARα agonist (24)],
3. treatment with probucol [PRO; maintained on chow containing 100 mg/kg/d probucol, an agent which increases fractional rate of LDL catabolism during cholesterol elimination. While probucol has moderate anti-oxidant properties, these appear to be a function of the LDL reducing effects of the drug rather than direct anti-oxidant effects (24)].
4. treatment with simvastatin [SIM: maintained on chow containing 20 mg/kg/d simvastatin, a cholesterol lowering agent via potent inhibition of HMG Co-A reductase (24,53), which also possesses anti-inflammatory properties associated with improved NO bioavailability (12,26,28)].
5. treatment with atorvastatin [ATOR; maintained on chow containing 10 mg/kg/d atorvastatin, a cholesterol lowering agent via potent inhibition of HMG Co-A reductase (24,53), which also possesses anti-inflammatory properties associated with improved NO bioavailability (4,25)]. The primary difference between SIM and ATOR may be that SIM has a greater capacity to elevate HDL-C than ATOR (9,24,28).

Rats were maintained on each of these groups for 3–4 weeks, 6–7 weeks or 10–11 weeks, at which time animals were used for experimentation (at 10, 13 and 17 weeks of age, respectively). On the day of the experiment, following an 8 hour fasting period, rats were anesthetized with injections of sodium pentobarbital (50 mg/kg, i.p.), and received tracheal intubation to facilitate maintenance of a patent airway. In all rats, a conduit artery was cannulated for determination of arterial pressure and for infusion of supplemental anesthetic and drugs, as necessary. Blood samples were drawn from the cannula for determination of glucose and insulin concentrations (Linco) as well as cholesterol and triglyceride levels (Waco). Plasma markers of inflammation were determined using commercially available ELISA systems (Luminex; Linco).

Preparation of Isolated Skeletal Muscle Resistance Arterioles

In all rats, the intramuscular continuation of the right gracilis arteriole was removed and cannulated (19). Within an individual group (above), vessels were divided into two sub-groups following an equilibration period. Group 1 examined dilator responses, where

NIH-PA Author Manuscript

NIH-PA Author Manuscript

NIH-PA Author Manuscript

arteriolar reactivity was evaluated in response to application of acetylcholine (10^{-10} M – 10^{-5} M) and sodium nitroprusside (10^{-6} M) to assess reactivity to NO from both endothelium-dependent and independent agonists, respectively. Subsequently, vessels were treated with TEMPOL (10^{-4} M) to assess the contribution of vascular oxidant tone to agonist-induced dilation. Group 2 examined constrictor reactivity, and mechanical responses were determined following challenge with phenylephrine (10^{-10} M – 10^{-7} M). Subsequently, vessels were treated with TEMPOL or L-NAME (10^{-4} M) to assess the contribution of vascular oxidant tone and endothelium-dependent NO production to the adrenergic constriction.

In all vessels, following the completion of the above procedures, the perfusate and superfusate were replaced with Ca^{2+}-free PSS and vessels were treated with 10^{-7} M phenylephrine until all tone was abolished. At this time, intralumenal pressure within the vessel was altered, in 20 mmHg increments, between 0 mmHg and 160 mmHg and the inner and outer diameter of arterioles was determined at each pressure. These data were used to calculate arteriolar wall mechanics which were used as indicators of structural alterations to the microvessel wall (2,20).

Measurement of Vascular NO Bioavailability

From a cohort of rats within the oldest group (17 weeks of age), the abdominal aorta was removed and vascular NO production was assessed using amperometric sensors (World Precision Instruments). Briefly, aortae were isolated, sectioned longitudinally, pinned in a silastic coated dish and superfused with warmed (37°C) PSS equilibrated with 95% O_2 and 5% CO_2. The NO sensor (ISO-NOPF 100) was placed in close apposition to the endothelial surface and a baseline level of current was obtained. Subsequently, increasing concentrations of methacholine (10^{-10}–10^{-6} M) were added to the bath and the changes in current were determined. To verify that responses represented NO release, these procedures were repeated following treatment of the aortic strip with L-NAME (10^{-4} M).

Histological Determination of Microvessel Density

At the conclusion of all muscle perfusion protocols, the gastrocnemius muscle from the left leg was removed, rinsed in PSS and fixed in 0.25% formalin. Muscles were embedded in paraffin and cut into 5 μm cross sections. Sections were incubated with *Griffonia simplicifolia* I lectin (Sigma), for subsequent determination of microvessel density (20,21).

Analyses of eNOS Expression and Activity

For determination of NOS expression, skeletal muscle arteries were homogenized and proteins within the homogenate were separated under denaturing conditions on an 8% SDS-polyacrilamide gel, after which proteins were transferred to a PVDF membrane and blocked. Subsequently, blots were incubated with mouse anti-eNOS/NOS Type III mAb (BD Transduction Laboratories), washed and incubated with appropriate horseradish peroxidase conjugated secondary antibody. GE Healthsciences ECL advance kits were used to visualize proteins. Additionally, in the oldest cohort of rats, the ascending and thoracic aorta, along with non-cannulated carotid, femoral, saphenous and iliac arteries were removed and frozen in liquid N_2, for the subsequent determination of NOS activity using a commercially available kit (Cayman).

Experimental Protocols

Initially, the right gracilis muscle resistance arteriole was removed for the evaluation of vascular reactivity and passive mechanical characteristics of the vessel wall, described above. Upon completion of these procedures, the right gastrocnemius muscle was removed,

NIH-PA Author Manuscript

NIH-PA Author Manuscript

NIH-PA Author Manuscript

cleared of non-muscular tissue, and its mass was determined. This muscle was then used for determination of microvessel density, as described above. Finally, the contralateral gastrocnemius muscle was removed for tissue banking and the aortic and arterial segments were removed for assessment of NO bioavailability and eNOS expression/activity, described above.

Data and Statistical Analyses

Mechanical responses of isolated arterioles following challenge with acetylcholine or phenylephrine were fit with the three-parameter logistic equation:

$$y=\min+\left[\frac{\max-\min}{1+10^{\log ED_{50}-x}}\right]$$

where y represents the change in arteriolar diameter, “min” and “max” represent the lower and upper bounds, respectively, of the change in arteriolar diameter with increasing agonist concentration, x is the logarithm of the agonist concentration and log ED_{50} represents the logarithm of the agonist concentration (x) at which the response (y) is halfway between the lower and upper bounds.

Data are presented as mean±SEM. Statistically significant differences in measured and calculated parameters in the present study were determined using analysis of variance (ANOVA). In all cases, Student-Newman-Keuls post hoc test was used when appropriate and $p<0.05$ was taken to reflect statistical significance. For analyses of inflammatory markers between groups, we employed discriminant techniques to eliminate the univariate nature of ANOVA and issues of independent variable co-linearity which minimizes the utility of regression techniques. Discriminant analyses are based on canonical correlation to maximize differences between *a priori* identified experimental groups. Multiple variables are arranged into structural equations based upon their *ceteris paribus* ability to distinguish those group differences. These stepwise analyses result in a rank ordering of correlation coefficients in terms of their significance for the establishment of differences between groups. These produce a series of algebraic functions which explain the differences between group centroids in the “x” dimension (Function 1), the “y” dimension (Function 2). Each function explains a specific percentage of the variance between the group centroids.

RESULTS

Table 1 presents basic characteristics of animal groups within the present study. OZR were consistently heavier than LZR, and this was not impacted by the anti-cholesterol therapies. While OZR ultimately developed a moderate hypertension as compared to LZR, the development of the elevated blood pressure was attenuated in OZR-SIM and OZR-ATOR groups. Fasting glucose was elevated in all OZR versus age matched LZR after 10 weeks of age, although glycemic control was improved in OZR-SIM and OZR-ATOR groups, as the level of blood glucose was associated with reduced plasma insulin with increasing age. The hypercholesterolemia in OZR was largely abolished as a result of the four anti-cholesterol therapies, and there was a modest blunting of the hypertriglyceridemia as a result of the PRO, SIM and ATOR treatments with age. Finally, plasma levels of nitrotyrosine were elevated with age in OZR versus LZR, indicative of a chronic elevation in oxidant stress, and this difference was blunted by chronic treatment with probucol, simvastatin and atorvastatin.

The changes to skeletal muscle microvessel density with time in LZR and OZR, and the impact of chronic treatment with the anti-cholesterol agents are summarized in Figure 1.

NIH-PA Author Manuscript

NIH-PA Author Manuscript

NIH-PA Author Manuscript

Microvessel density was not significantly impacted by the evolution of the metabolic syndrome at 7 weeks of age between LZR and OZR (Panel A), and as such, none of the pharmacological treatments impacted this relationship. However, with increasing severity of the metabolic syndrome over time, the degree of microvascular rarefaction was increased between OZR and LZR (Panels B–D). Chronic treatment with GEM and PRO had minor impacts on rarefaction in OZR, despite their effectiveness in reducing total cholesterol. In contrast, chronic treatment with either SIM or ATOR was effective at delaying/blunting the progression of microvascular rarefaction in OZR at 10, 13 and 17 weeks of age.

At both 7 (Panel A) and 10 weeks (Panel B) of age, regardless of experimental group, both the arteriolar incremental distensibility and the circumferential stress versus strain relationship (panel inset) was not different between LZR and OZR (Figure 2). However, in both 13 week (Panel C) and 17 week (Panel D) old OZR, the slope coefficient describing this parameter was significantly elevated in OZR as compared to LZR under control conditions. While the anti-cholesterol therapies did not significantly impact this shift in the stress versus strain relationship between arterioles of LZR and OZR at 13 weeks of age, treatment with SIM or ATOR blunted this difference at 17 weeks of age, such that the slope coefficients exhibited an intermediate phenotype between that for untreated LZR and OZR.

Data describing arteriolar dilation in response to challenge with acetylcholine and the impact of acute treatment of vessels with TEMPOL on the upper bound of this relationship are summarized in Figure 3. At 7 weeks of age, the acetylcholine-induced dilator reactivity of resistance arterioles from LZR and OZR was comparable, regardless of experimental groups (Panel A) and the impact of anti-oxidant treatment on this response was negligible (Panel B). A similar situation is present at 10 weeks of age, although separation in the acetylcholine-induced dilation of resistance arterioles, while not statistically significant between LZR and OZR, is becoming apparent (Panel C). However, by 13 weeks of age (Panels E and F), and even more evident at 17 weeks of age (Panels G and H), acetylcholine-induced dilation was significantly reduced in OZR versus LZR, and this separation was blunted by treatment with SIM and ATOR. The impact of TEMPOL treatment on this response also began to demonstrate differences, as treatment of arterioles from OZR and OZR-GEM with the anti-oxidant resulted in a significant improvement in the upper bound of the acetylcholine-induced response. In all cases, treatment of vessels with L-NAME abolished arteriolar responses to acetylcholine, and arteriolar dilation in response to challenge with sodium nitroprusside was not different between groups (data not shown).

Regardless of the pharmacological intervention imposed, arterial expression of eNOS between LZR and OZR did not demonstrate a consistent or significant difference between or within the two strains. Further, there was no evidence of a consistent or significant impact of age on eNOS expression between LZR and OZR (data not shown).

Figure 4 summarizes arterial eNOS activity and methacholine-induced NO production in the oldest cohort of LZR and OZR under the conditions of the present study. At 17 weeks of age, eNOS activity (Panel A) was not significantly different between LZR and OZR, and treatment with the anti-cholesterol therapies was without consistent effect. Additionally, methacholine-induced production of NO from arterial strips, assessed using amperometric sensors, was attenuated in OZR versus LZR (Panel B), although chronic ingestion of SIM or ATOR increased NO production in response to challenge with methacholine in OZR.

Data describing arteriolar constrictor responses in vessels from LZR and OZR following challenge with phenylephrine under the conditions of the present study are summarized in Figure 5. At 7 (Panel A) and 10 (Panel C) weeks of age, challenge with increasing concentrations of phenylephrine produced similar arteriolar constrictor response in OZR

NIH-PA Author Manuscript

NIH-PA Author Manuscript

NIH-PA Author Manuscript

versus LZR under control conditions, and this relationship was not impacted by any of the anti-cholesterol therapies. Further, inhibition of eNOS enzymes with L-NAME had no impact on these responses at either 7 weeks (Panel B) or 10 weeks (Panel D) of age. However, by 13 weeks of age, OZR began to exhibit an increased constrictor response to phenylephrine (Panel E), and this effect was even more pronounced at 17 weeks of age (Panel G). This increased constrictor response was largely unaltered by chronic treatment with GEM or PRO at either age, although chronic treatment with SIM and ATOR blunted the augmentation to phenylephrine-induced constriction with age in OZR. Acute inhibition of eNOS with L-NAME had no effect on the differences in phenylephrine-induced constriction at 13 (Panel F) and 17 (Panel H) weeks of age between LZR and OZR under control conditions or following chronic treatment with GEM, but attenuated the impact of SIM and ATOR on moderating the increased adrenergic reactivity in OZR with age. Acute application of phentolamine (10^{-5} M) abolished all arteriolar responses to phenylephrine (data not shown).

Data describing the changes in plasma markers of inflammation across groups are summarized in Table 2. As compared to marker concentration in LZR, OZR demonstrated significant elevations in plasma concentrations of IL-1β, IL-6, IL-10, TNF-α, RANTES, MCP-1 and VEGF between 7 and 17 weeks of age. In general, GEM treatment had a minimal impact on these relationships in OZR, regardless of animal age, and PRO treatment reduced the elevation in RANTES (regulated upon activation normal T-cell expressed and secreted) at 17 weeks only. In contrast, treatment of OZR with SIM or ATOR altered levels of all markers by 13 weeks of age, except VEGF, such that their plasma concentration was significantly different from that in OZR under control conditions. Regardless of treatment, plasma concentrations of VEGF were elevated in OZR versus LZR.

Figure 6 summarizes data from 17 week old animals from all experimental groups correlating gastrocnemius muscle microvessel density with plasma total cholesterol (Panel A) or vascular NO bioavailability (Panel B), with values from individual animals being presented. As evident from Panel A, plasma total cholesterol is a poor predictor of rarefaction and does not effectively explain the variability in muscle vascularity in the present study. In contrast, NO bioavailability, estimated from the magnitude of the upper bound from the three parameter logistic equation describing the acetylcholine concentration-response curve for individual arterioles, was a much stronger predictor of muscle vascularity, as this parameter explained almost 81% of the variability in vessel density in the present study. This relationship is evident at other ages as well (data not shown).

Table 3 presents the results of stepwise discriminant analysis based on inflammatory marker data across the experimental groups. These analyses suggest that, while most measured markers of inflammation were well correlated with microvessel density and NO bioavailability, IL-10 and MCP-1 were consistent contributors to differences not only across the experimental groups, but also over time within individual groups. In contrast, plasma RANTES levels became increasingly significant with time in terms of discriminating between groups. Alternatively, plasma TNF-α, demonstrated an inverse relationship, become less significant with time, to the point where it dropped out of the model entirely. These data are presented graphically in Figure 7. Plasma levels of VEGF, IL-6 and IL-1β, while well correlated with microvessel density based on univariate analyses did not contribute to the ability to discriminate between groups, and as such are not presented in Table 3.

The relationships between these identified markers, NO bioavailability and microvessel density between 17 week old LZR and OZR is presented in Figure 8. RANTES (Panel A),

NIH-PA Author Manuscript

NIH-PA Author Manuscript

NIH-PA Author Manuscript

IL-10 (Panel B), MCP-1 (Panel C), and TNF-α (Panel D) all demonstrate a strong correlation with NO bioavailability and microvessel density across the animal groups.

DISCUSSION

As a contributing component to the metabolic syndrome, OZR develop moderate hypercholesterolemia, in addition to other co-morbidities associated with this multi-pathology state. While previous studies have suggested that elevated plasma cholesterol can be associated with reduced capillary density (7,42) and blunted angiogenic responses (36,45), it is presently unclear as to the contribution of inflammatory status in terms of mediating these effects. Given this, the present study was designed to chronically treat OZR with multiple mechanistically distinct anti-cholesterol therapies throughout the period in which microvessel loss is established to better distinguish the role for plasma cholesterol in terms of its contribution to skeletal muscle microvascular rarefaction, and the role of chronic inflammation in this process.

The most immediate observation of the current study was that treatment of OZR with the anti-cholesterol agents all resulted in a comparable reduction in hypercholesterolemia at each age, despite mechanistically divergent routes of action. Probucol lowers cholesterol by increasing the fractional rate of LDL catabolism in the metabolic pathway for cholesterol elimination from the body, and may inhibit early stages of cholesterol biosynthesis (24). Gemfibrozil, a fibric acid derivative, is a PPARα agonist and can reduce plasma LDL through multiple routes, including cholesteryl ester transfer protein activity, an increased binding affinity of LDL to its receptors, and an increased expression of hepatic LDL receptors (24). Atorvastatin and simvastatin are HMG CoA reductase inhibitors, and as such exert their anti-cholesterol actions via an inhibition of this rate limiting step in cholesterol biosynthesis. This inhibition of hepatic cholesterologenesis results in an increased expression of hepatic LDL receptors, and leads to lowered circulating cholesterol levels (24,27).

Although each of these therapies was comparable in terms of efficacy in reducing plasma total cholesterol, considerable divergence was evident for their ability to ameliorate microvascular rarefaction and improve arteriolar reactivity. From a structural perspective, despite reductions in total cholesterol, treatment with gemfibrozil (and to a lesser extent probucol) had a minimal impact on blunting microvascular rarefaction with age in OZR. In contrast, chronic statin therapy lessened the severity of rarefaction, such that microvessel density assumed a level that, although reduced from LZR, was consistently improved versus untreated OZR. This observation is intriguing in that recent studies have identified a biphasic, lipid-independent, effect of chronic statin therapy on microvessel density. Specifically, it may be that low-dose statin therapy is associated with a “pro-angiogenic” environment through activation of Akt and increased NO bioavailability, whereas higher statin doses can cause angiostatic effects which are potentially mediated through a decreased protein prenylation and an inhibition of cell growth (4,37,39,49). With regard to mechanics of the microvessel wall in OZR, an ameliorative effect was also identified, as the severe reduction in wall distensibility in OZR was modestly attenuated as a result of chronic ingestion of atorvastatin or simvastatin, with lesser impacts from probucol or gemfibrozil. These results support those determined previously, as statin therapy has been effective in reducing wall stiffness in hypercholesterolemia (38,40), although additional studies have suggested that this effect may be independent of lipid profiles (44), and may better represent the pleiotropic effects of statins on endothelial function or inflammatory status.

In our previous studies, we have provided evidence suggesting one of the main causative mechanisms associated with microvascular rarefaction in OZR may be a chronic reduction

NIH-PA Author Manuscript

NIH-PA Author Manuscript

NIH-PA Author Manuscript

in vascular NO bioavailability (16). The present results support this hypothesis, as both vascular reactivity to acetylcholine (Figure 3) and methacholine-induced NO production (Figure 4) were improved with statin therapy in OZR. Further, when data from an age cohort of animals are summarized, an index of vascular NO bioavailability (upper bound of the acetylcholine concentration-dilator response relationship) was a strong predictor of gastrocnemius muscle microvessel density (Figure 6).

The increased vascular NO bioavailability as a result of chronic atorvastatin or simvastatin treatment was also evident with regard to phenylephrine-induced constrictor reactivity. Specifically, the increased constrictor response of arterioles of OZR (versus LZR) in response to adrenergic stimulation was not impacted by chronic anti-cholesterol therapy with gemfibrozil. However, chronic treatment of OZR with atorvastatin, simvastatin or probucol blunted the upper bound of this response, although responses were still increased versus those in LZR. This may have been due to an increased vascular NO bioavailability, as acute application of L-NAME, while having minimal impact on phenylephrine-induced arteriolar constriction in OZR (±gemfibrozil), increased the upper bound of this relationship in OZR treated with either of the other three agents. These data clearly suggest that chronic treatment with anti-cholesterol agents of the “statin” family will increase the vascular NO bioavailability (and reduce vascular oxidant stress) in OZR, and that this relationship can impact both vascular reactivity (both dilator and constrictor) and microvascular network structure.

One of the profound implications for hypercholesterolemia is the genesis of an elevated state of inflammation (8,29,30), that can be associated with evolution of peripheral vasculopathy (34,41,46). While inherent in the treatment of hypercholesterolemia is a reduction of plasma cholesterol, amelioration of inflammation, and improved outcomes, a key observation from the present study was that although each treatment was effective in reducing cholesterol in OZR, there was a considerable disparity in terms of these other processes. In the OZR model of the metabolic syndrome, we (13) and others (1,33) have clearly demonstrated an elevated state of inflammation and that specific markers of inflammation can be strongly correlated with vascular outcomes (positively or negatively, depending on marker and outcome). As the metabolic syndrome is, by definition, composed of multiple pro-inflammatory pathologies (8), changes in multiple markers of inflammation between groups were each significant (Table 2). Further, given that indices of microvascular dysfunction were also tightly associated with animal group, as well as NO bioavailability and inflammatory state severity, significant correlations were also determined between individual markers of inflammation and specific indices of vascular dysfunction. While interesting from a conceptual standpoint, these results are largely uninformative with respect to evaluating mechanistic bases of inflammation-induced vascular dysfunction in OZR. Further, additional insight cannot effectively be gleaned from multivariate regression techniques, as the independent variables (i.e., markers of inflammation) demonstrate a greater co-linearity amongst themselves than with an outcome (e.g., microvessel density).

As a result, we incorporated the use of discriminant analyses (Figure 7 and Table 3), a classification technique for evaluating how multiple variables contribute to differences between experimental groups and one which is specifically designed for accurate hypothesis development. These analyses result in a rank ordering of *ceteris paribus* correlation coefficients in terms of significance for the establishment of differences between groups. The beneficial impact of discriminant analyses is that through a series of iterations, we are able to identify which parameters are most significant, and also which parameters are significant only because they operate through the magnitude of others. As an example, while results from ANOVA or regression suggest that IL-1β or IL-6 are correlated with low NO bioavailability, they suffer from considerably co-linearity with other predictive markers,

NIH-PA Author Manuscript

NIH-PA Author Manuscript

NIH-PA Author Manuscript

limiting their utility. In contrast, discriminant analyses suggests that these markers may be less important than RANTES, MCP-1, IL-10, and TNF-α, and may not directly contribute to differences between LZR and OZR under control conditions and following chronic anti-cholesterol therapy. These parameters identified from discriminant analyses can be used for the more targeted model development and future hypothesis testing. It is important to emphasize that these procedures do not result in an identification of the four key markers contributing to vasculopathy in the metabolic syndrome. Rather, given the limited data set employed in the present study, these analyses indicate how four markers, each of which demonstrates a strong univariate association with the vascular outcomes vary over time in terms of their ability to discriminate an outcome between experimental groups. With ongoing study and the inclusion of additional discriminating elements, the results of these procedures will change, although the ultimate goal is the convergence on a more stable predictive model with increasing iterations.

One of the interesting observations of the present study was while chronic treatment with the anti-cholesterol agents reduced total cholesterol in OZR to levels that were comparable to that in LZR, treatment with either of the two statin medications had the additional benefit of also reducing mean arterial pressure and improving glycemic control (i.e., insulin sensitivity) as well as providing a modest lowering of the hypertriglyceridemia in OZR. Given that the statin medications were also the most effective in terms of improving microvascular outcomes in the present study, it may be that the combination of these associated beneficial impacts of statin therapy on the other contributing pathologies of the metabolic syndrome in OZR also represented substantial mediators of the improvement to microvascular function. While an appealing possibility, the current data only allow for speculation on this hypothesis, as additional control experiments would be required to evaluate the role for these additional elements. However, this is an area of investigation that may warrant additional investment.

In summary, while development of moderate hypercholesterolemia in OZR is associated with impaired microvascular function, chronic treatment of elevated cholesterol levels does not *per se* result in a significant improvement to poor outcomes. Rather, only anti-cholesterol treatments that improved vascular NO bioavailability and attenuated the chronic inflammation in OZR (statins) were successful in improving microvascular and perfusion outcomes, suggesting that total plasma cholesterol itself may be a poor predictor of vascular outcomes in this model. Chronic inflammation, when combined with vascular NO bioavailability, may be far stronger than total cholesterol as a predictor of vascular dysfunction, and the implementation of discriminant analyses for changes to the inflammatory profile may reflect a more informative means through which future experiments may be designed.

Acknowledgments

Support: American Heart Association (SDG 0330194N; EIA 0740129N) and NIH (R01 DK64668).

REFERENCES

1. Barbato JE, Zuckerbraun BS, Overhaus M, Raman KG, Tzeng E. Nitric oxide modulates vascular inflammation and intimal hyperplasia in insulin resistance and the metabolic syndrome. Am J Physiol Heart Circ Physiol. 2005; 289:H228–236. [PubMed: 15734883]
2. Baumbach GL, Hajdu MA. Mechanics and composition of cerebral arterioles in renal and spontaneously hypertensive rats. Hypertension. 1993; 21:816–826. [PubMed: 8500863]
3. Beckman JA, Creager MA. The nonlipid effects of statins on endothelial function. Trends Cardiovasc Med. 2006; 16:156–162. [PubMed: 16781949]

NIH-PA Author Manuscript

NIH-PA Author Manuscript

NIH-PA Author Manuscript

4. Boodhwani M, Nakai Y, Voisine P, Feng J, Li J, Mieno S, Ramlawi B, Bianchi C, Laham R, Sellke FW. High-dose atorvastatin improves hypercholesterolemic coronary endothelial dysfunction without improving the angiogenic response. Circulation. 2006; 114:I402–I408. [PubMed: 16820608]
5. Bray GA. The Zucker-fatty rat: a review. Fed Proc. 1977; 36:148–153. [PubMed: 320051]
6. Brzezinska AK, Gebremedhin D, Chilian WM, Kalyanaraman B, Elliott SJ. Peroxynitrite reversibly inhibits Ca(2+)-activated K(+) channels in rat cerebral artery smooth muscle cells. Am J Physiol Heart Circ Physiol. 2000; 278:H1883–H1890. [PubMed: 10843885]
7. Bucay M, Nguy J, Barrios R, Chen CH, Henry PD. Impaired adaptive vascular growth in hypercholesterolemic rabbit. Atherosclerosis. 1998; 139:243–251. [PubMed: 9712330]
8. Dandona P, Aljada A, Chaudhuri A, Mohanty P, Garg R. Metabolic syndrome: a comprehensive perspective based on interactions between obesity, diabetes, and inflammation. Circulation. 2005; 111:1448–1454. [PubMed: 15781756]
9. Davidson MH, Ose L, Frohlich J, Scott RS, Dujovne CA, Escobar ID, Bertolami MC, Cihon F, Maccubbin DL, Mercuri M. Differential effects of simvastatin and atorvastatin on high-density lipoprotein cholesterol and apolipoprotein A-I are consistent across hypercholesterolemic patient subgroups. Clin Cardiol. 2003; 26:509–514. [PubMed: 14640465]
10. Duarte J, Martinez A, Bermejo A, Vera B, Gamez MJ, Cabo P, Zarzuelo A. Cardiovascular effects of captopril and enalapril in obese Zucker rats. Eur J Pharmacol. 1999; 365:225–232. [PubMed: 9988106]
11. Endres M. Statins: potential new indications in inflammatory conditions. Atheroscler Suppl. 2006; 7:31–35. [PubMed: 16503422]
12. Field KM. Effect of 3-hydroxy-3-methylglutaryl coenzyme A reductase inhibitors on high-sensitivity C-reactive protein levels. Pharmacotherapy. 2005; 25:1365–1377. [PubMed: 16185181]
13. Frisbee JC, Balch Samora J, Peterson J, Bryner R. Exercise training blunts microvascular rarefaction in the metabolic syndrome. Am J Physiol Heart Circ Physiol. 2006; 291:H2483–H2492. [PubMed: 16798823]
14. Frisbee JC. Impaired hemorrhage tolerance in the obese Zucker rat model of metabolic syndrome. J Appl Physiol. 2006; 100:465–473. [PubMed: 16223976]
15. Frisbee JC. Vascular adrenergic tone and structural narrowing constrain reactive hyperemia in skeletal muscle of obese Zucker rats. Am J Physiol Heart Circ Physiol. 2006; 290:H2066–H2074. [PubMed: 16373580]
16. Frisbee JC. Reduced nitric oxide bioavailability contributes to skeletal muscle microvessel rarefaction in the metabolic syndrome. Am J Physiol Regul Integr Comp Physiol. 2005; 289:R307–R316. [PubMed: 15802560]
17. Frisbee JC. Hypertension-independent microvascular rarefaction in the obese Zucker rat model of the metabolic syndrome. Microcirculation. 2005; 12:383–392. [PubMed: 16020387]
18. Frisbee JC. Enhanced arteriolar alpha-adrenergic constriction impairs dilator responses and skeletal muscle perfusion in obese Zucker rats. J Appl Physiol. 2004; 97:764–772. [PubMed: 15075303]
19. Frisbee JC. Impaired skeletal muscle perfusion in obese Zucker rats. Am J Physiol Regul Integr Comp Physiol. 2003; 285:R1124–R1134. [PubMed: 12855417]
20. Frisbee JC. Remodeling of the skeletal muscle microcirculation increases resistance to perfusion in obese Zucker rats. Am J Physiol Heart Circ Physiol. 2003; 285:H104–H111. [PubMed: 12649071]
21. Ginsberg HN. Efficacy and mechanisms of action of statins in the treatment of diabetic dyslipidemia. J Clin Endocrinol Metab. 2006; 91:383–392. [PubMed: 16291700]
22. Greene AS, Lombard JH, Cowley AW Jr, Hansen-Smith FM. Microvessel changes in hypertension measured by Griffonia simplicifolia I lectin. Hypertension. 1990; 15:779–783. [PubMed: 2351431]
23. Guerre-Millo M. Regulation of ob gene and overexpression in obesity. Biomed Pharmacother. 1997; 51:318–323. [PubMed: 9436523]
24. Hardman, JG.; Limbird, LE.; Gilman, AG., editors. Goodman and Gilman's: The Pharmacological Basis of Therapeutics. 10th edition. McGraw-Hill, Inc.; New York, NY: 2001. p. 971-1002.

NIH-PA Author Manuscript

NIH-PA Author Manuscript

NIH-PA Author Manuscript

25. Hognestad A, Aukrust P, Wergeland R, Stokke O, Gullestad L, Semb AG, Holm T, Andreassen AK, Kjekshus JK. Effects of conventional and aggressive statin treatment on markers of endothelial function and inflammation. Clin Cardiol. 2004; 27:199–203. [PubMed: 15119693]
26. John S, Delles C, Jacobi J, Schlaich MP, Schneider M, Schmitz G, Schmieder RE. Rapid improvement of nitric oxide bioavailability after lipid-lowering therapy with cerivastatin within two weeks. J Am Coll Cardiol. 2001; 37:1351–1358. [PubMed: 11300446]
27. Knopp RH, Paramsothy P. Treatment of hypercholesterolemia in patients with metabolic syndrome: how do different statins compare? Nat Clin Pract Endocrinol Metab. 2006; 2:136–137. [PubMed: 16932272]
28. Laufs U, La Fata V, Plutzky J, Liao JK. Upregulation of endothelial nitric oxide synthase by HMG CoA reductase inhibitors. Circulation. 1998; 97:1129–1135. [PubMed: 9537338]
29. Libby P. Inflammation in atherosclerosis. Nature. 2002; 420:868–874. [PubMed: 12490960]
30. Lyon CJ, Law RE, Hsueh WA. Minireview: adiposity, inflammation, and atherogenesis. Endocrinology. 2003; 144:2195–2200. [PubMed: 12746274]
31. Martinez-Gonzalez J, Alfon J, Berrozpe M, Badimon L. HMG-CoA reductase inhibitors reduce vascular monocyte chemotactic protein-1 expression in early lesions from hypercholesterolemic swine independently of their effect on plasma cholesterol levels. Atherosclerosis. 2001; 159:27–33. [PubMed: 11689203]
32. Mason RP, Walter MF, Day CA, Jacob RF. Intermolecular differences of 3-hydroxy-3-methylglutaryl coenzyme a reductase inhibitors contribute to distinct pharmacologic and pleiotropic actions. Am J Cardiol. 2005; 96:11F–23F.
33. Picchi A, Gao X, Belmadani S, Potter BJ, Focardi M, Chilian WM, Zhang C. Tumor necrosis factor-alpha induces endothelial dysfunction in the prediabetic metabolic syndrome. Circ Res. 2006; 99:69–77. [PubMed: 16741160]
34. Pirro M, Schillaci G, Savarese G, Gemelli F, Vaudo G, Siepi D, Bagaglia F, Mannarino E. Low-grade systemic inflammation impairs arterial stiffness in newly diagnosed hypercholesterolaemia. Eur J Clin Invest. 2004; 34:335–341. [PubMed: 15147330]
35. Ray KK, Cannon CP. The potential relevance of the multiple lipid-independent (pleiotropic) effects of statins in the management of acute coronary syndromes. J Am Coll Cardiol. 2005; 46:1425–1433. [PubMed: 16226165]
36. Sasaki K, Duan J, Murohara T, Ikeda H, Shintani S, Shimada T, Akita T, Egami K, Imaizumi T. Rescue of hypercholesterolemia-related impairment of angiogenesis by oral folate supplementation. J Am Coll Cardiol. 2003; 42:364–372. [PubMed: 12875777]
37. Sata M, Nishimatsu H, Osuga J, Tanaka K, Ishizaka N, Ishibashi S, Hirata Y, Nagai R. Statins augment collateral growth in response to ischemia but they do not promote cancer and atherosclerosis. Hypertension. 2004; 43:1214–1220. [PubMed: 15166180]
38. Shige H, Dart A, Nestel P. Simvastatin improves arterial compliance in the lower limb but not in the aorta. Atherosclerosis. 2001; 155:245–250. [PubMed: 11223448]
39. Skaletz-Rorowski A, Walsh K. Statin therapy and angiogenesis. Curr Opin Lipidol. 2003; 14:599–603. [PubMed: 14624137]
40. Smilde TJ, van den Berkmortel FW, Wollersheim H, van Langen H, Kastelein JJ, Stalenhoef AF. The effect of cholesterol lowering on carotid and femoral artery wall stiffness and thickness in patients with familial hypercholesterolaemia. Eur J Clin Invest. 2000; 30:473–480. [PubMed: 10849014]
41. Stokes KY. Microvascular responses to hypercholesterolemia: the interactions between innate and adaptive immune responses. Antioxid Redox Signal. 2006; 8:1141–1151. [PubMed: 16910762]
42. Theilmeier G, Verhamme P, Dymarkowski S, Beck H, Bernar H, Lox M, Janssens S, Herregods MC, Verbeken E, Collen D, Plate K, Flameng W, Holvoet P. Hypercholesterolemia in minipigs impairs left ventricular response to stress: association with decreased coronary flow reserve and reduced capillary density. Circulation. 2002; 106:1140–1146. [PubMed: 12196342]
43. Tofovic SP, Jackson EK. Rat models of the metabolic syndrome. Methods Mol Med. 2003; 86:29–46. [PubMed: 12886760]

NIH-PA Author Manuscript

NIH-PA Author Manuscript

NIH-PA Author Manuscript

44. Ubels FL, Muntinga JH, van Doormaal JJ, Reitsma WD, Smit AJ. Effects of initial and long-term lipid-lowering therapy on vascular wall characteristics. Atherosclerosis. 2001; 154:155–161. [PubMed: 11137095]
45. Van Belle E, Rivard A, Chen D, Silver M, Bunting S, Ferrara N, Symes JF, Bauters C, Isner JM. Hypercholesterolemia attenuates angiogenesis but does not preclude augmentation by angiogenic cytokines. Circulation. 1997; 96:2667–2674. [PubMed: 9355908]
46. van Haelst PL, van Doormaal JJ, Asselbergs FW, van Roon AM, Veeger NJ, Henneman MM, Smit AJ, Tervaert JW, May JF, Gans RO. Correlates of endothelial function and their relationship with inflammation in patients with familial hypercholesterolaemia. Clin Sci (Lond). 2003; 104:627–632. [PubMed: 12558496]
47. Vaziri ND, Xu ZG, Shahkarami A, Huang KT, Rodriguez-Iturbe B, Natarajan R. Role of AT-1 receptor in regulation of vascular MCP-1, IL-6, PAI-1, MAP kinase, and matrix expressions in obesity. Kidney Int. 2005; 68:2787–2793. [PubMed: 16316354]
48. Walker AB, Chattington PD, Buckingham RE, Williams G. The thiazolidinedione rosiglitazone (BRL-49653) lowers blood pressure and protects against impairment of endothelial function in Zucker fatty rats. Diabetes. 1999; 48:1448–1453. [PubMed: 10389852]
49. Weis M, Heeschen C, Glassford AJ, Cooke JP. Statins have biphasic effects on angiogenesis. Circulation. 2002; 105:739–745. [PubMed: 11839631]
50. Xiang L, Naik JS, Abram SR, Hester RL. Chronic hyperglycemia impairs functional vasodilation via increasing thromboxane receptor-mediated vasoconstriction. Am J Physiol Heart Circ Physiol. 2006 Epub ahead of print.
51. Xiang L, Naik JS, Hodnett BL, Hester RL. Altered arachidonic acid metabolism impairs functional vasodilation in metabolic syndrome. Am J Physiol Regul Integr Comp Physiol. 2006; 290:R134–R138. [PubMed: 16166209]
52. Xiang L, Naik J, Hester RL. Exercise-induced increase in skeletal muscle vasodilatory responses in obese Zucker rats. Am J Physiol Regul Integr Comp Physiol. 2005; 288:R987–R991. [PubMed: 15604297]
53. Zhou Z, Rahme E, Pilote L. Are statins created equal? Evidence from randomized trials of pravastatin, simvastatin, and atorvastatin for cardiovascular disease prevention. Am Heart J. 2006; 151:273–281. [PubMed: 16442888]

NIH-PA Author Manuscript

NIH-PA Author Manuscript

NIH-PA Author Manuscript

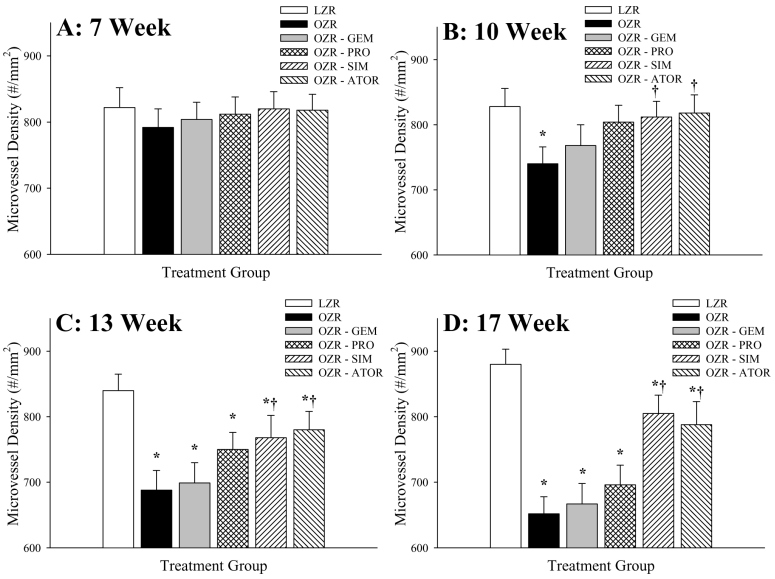

Figure 1.

Data (mean±SEM) microvessel density within skeletal muscle of LZR and OZR at 7 weeks (Panel A), 10 weeks (Panel B), 13 weeks (Panel C) and 17 weeks (Panel D) of age. Microvessel density data are presented under control conditions and following chronic treatment of OZR with the anti-cholesterol therapies: gemfibrozil, probucol, simvastatin or atorvastatin. Microvessel density was determined using fluorescence microscopy following labeling of microvessel with *Griffonia simplicifolia* I lectin (please see text for details). * $p<0.05$ vs. LZR; † $p<0.05$ vs. OZR.

NIH-PA Author Manuscript

NIH-PA Author Manuscript

NIH-PA Author Manuscript

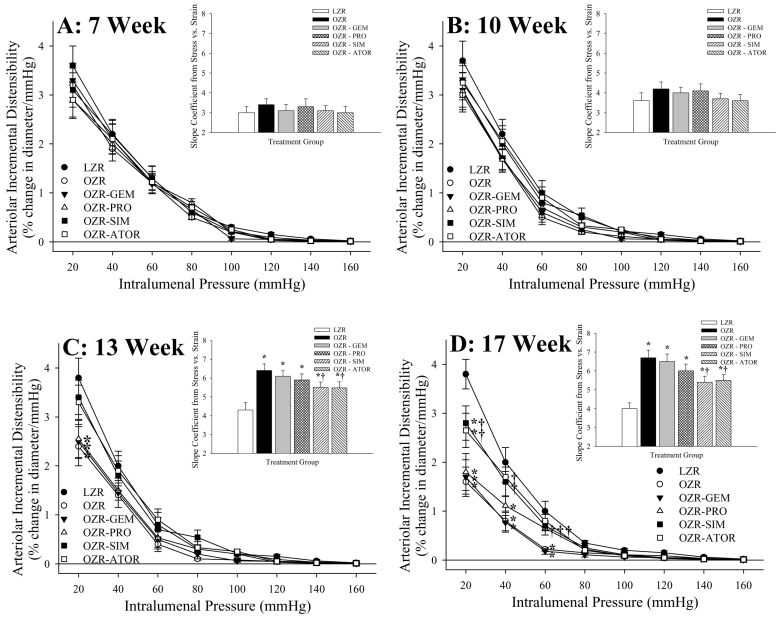

Figure 2.

Data (mean±SEM) describing incremental distensibility and the slope (β) coefficients from circumferential stress versus strain relationships (inset panels) of skeletal muscle arterioles of LZR and OZR at 7 weeks (Panel A), 10 weeks (Panel B), 13 weeks (Panel C) and 17 weeks (Panel D) of age. Arteriolar wall mechanics data are presented control conditions and following chronic treatment of OZR with the anti-cholesterol therapies: gemfibrozil, probucol, simvastatin or atorvastatin. * $p<0.05$ vs. LZR; † $p<0.05$ vs. OZR.

NIH-PA Author Manuscript
NIH-PA Author Manuscript
NIH-PA Author Manuscript

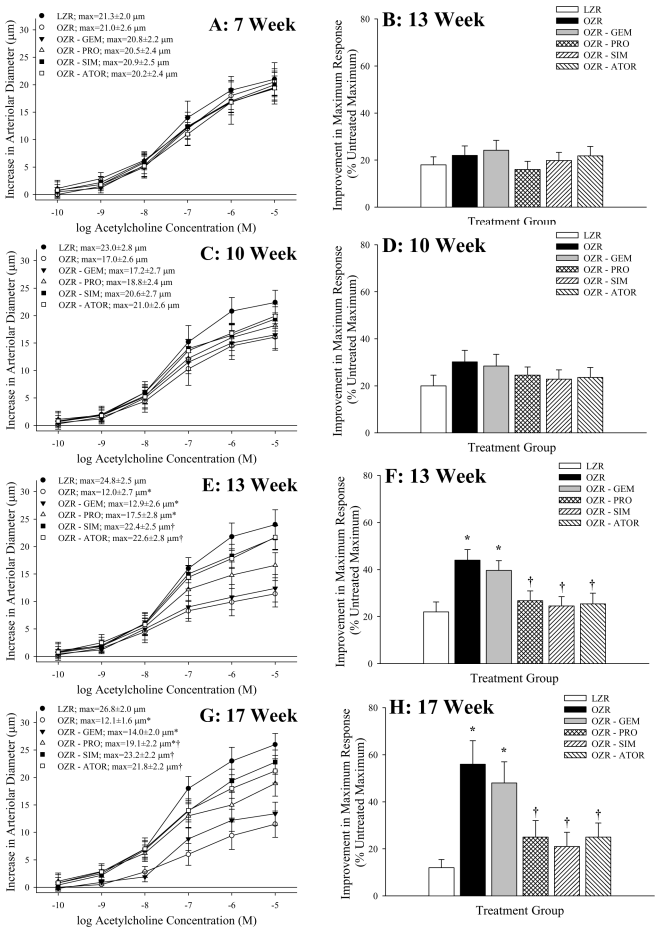

Figure 3.

Data (mean±SEM) describing skeletal muscle arteriolar dilation in response to increasing concentrations of acetylcholine of LZR and OZR under control conditions and following chronic treatment of OZR with gemfibrozil, probucol, simvastatin or atorvastatin. Data area presented as paired panels, with the left panels summarizing the concentration-response relationship, and the right panel presenting the contribution of oxidant stress in terms of impacting acetylcholine-induced dilation where the change in the upper bound of this relationship is shown following treatment of the arteriole with TEMPOL. Data are presented for animals at 7 weeks (Panels A/B), 10 weeks (Panels C/D), 13 weeks (Panels E/F) and 17 weeks (Panels G/H) of age. * $p<0.05$ vs. LZR; † $p<0.05$ vs. OZR.

NIH-PA Author Manuscript
NIH-PA Author Manuscript
NIH-PA Author Manuscript

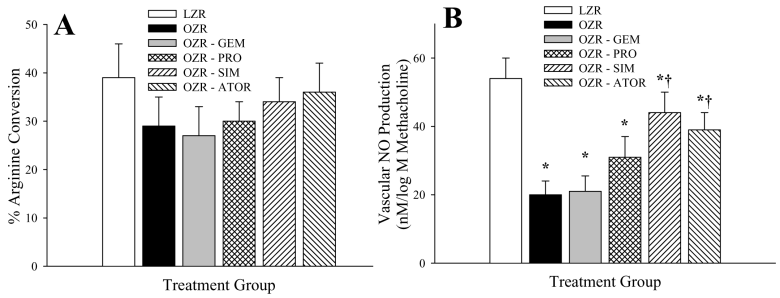

Figure 4.

Vascular eNOS activity (Panel A; presented as the % arginine conversion), and methacholine-induced NO bioavailability (Panel B; where data present the slope of the relationship between vascular NO production and methacholine concentration, nM/log M methacholine) in LZR and OZR at 17 weeks of age. Data (presented as mean±SEM) are summarized for LZR and OZR under control conditions and following chronic treatment of OZR with gemfibrozil, probucol, simvastatin or atorvastatin. * $p<0.05$ vs. LZR; † $p<0.05$ vs. OZR.

NIH-PA Author Manuscript
NIH-PA Author Manuscript
NIH-PA Author Manuscript

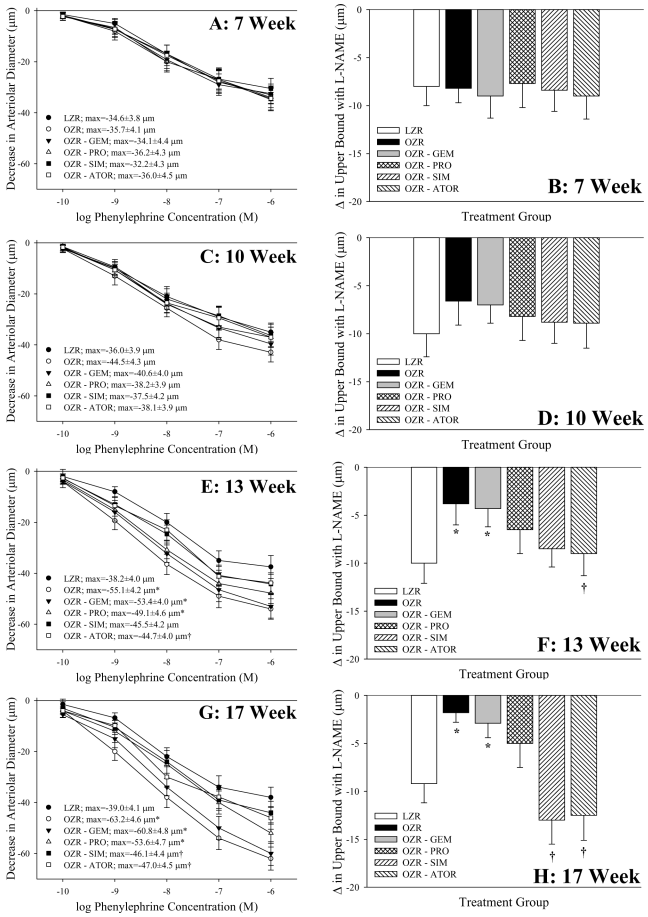

Figure 5.

Data (mean±SEM) describing skeletal muscle arteriolar constriction in response to increasing concentrations of phenylephrine in LZR and OZR under control conditions and following chronic treatment of OZR with gemfibrozil, probucol, simvastatin or atorvastatin. Data area presented as paired panels, with the left panels summarizing the concentration-response relationship, and the right panel presenting the contribution of vascular nitric oxide production in terms of impacting phenylephrine-induced constriction where the change in the upper bound of this relationship is shown following treatment of the arteriole with L-NAME. Data are presented for animals at 7 weeks (Panels A/B), 10 weeks (Panels C/D), 13 weeks (Panels E/F) and 17 weeks (Panels G/H) of age. * $p<0.05$ vs. LZR; † $p<0.05$ vs. OZR.

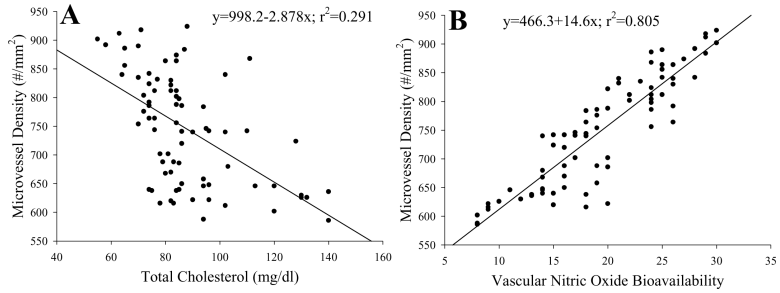

Figure 6.

The relation between plasma total cholesterol level (Panel A), or a proxy variable for NO bioavailability (upper bound of the acetylcholine dose-response relationship; Panel B), and microvessel density from the different animals in the present study. Each animal used in the study, across the experimental groups is presented in this figure. The inset text presents the linear regression equation that best fits these data and the degree to which that equation explains the variability in the data.

NIH-PA Author Manuscript NIH-PA Author Manuscript NIH-PA Author Manuscript

NIH-PA Author Manuscript
NIH-PA Author Manuscript
NIH-PA Author Manuscript

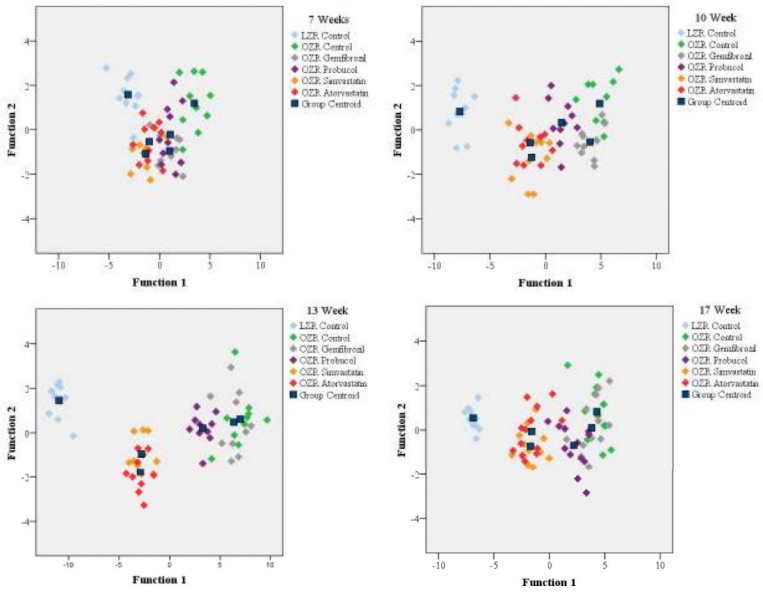

Figure 7.

Summary plot for the results of the discriminant analyses in the present study. These results provide the functions 1 and 2 (presented in Table 3) which contribute the majority (>90%) of the differences between the experimental groups at each age. Specifically, RANTES, IL-10, MCP-1 and TNF-α play the greatest role in terms of establishing differences between LZR (light blue), OZR (green), and OZR under the four treatment conditions of the present study; gemfibrozil (grey), probucol (purple), simvastatin (orange) and atorvastatin (red). The centroids for each group are presented in the dark blue squares.

NIH-PA Author Manuscript

NIH-PA Author Manuscript

NIH-PA Author Manuscript

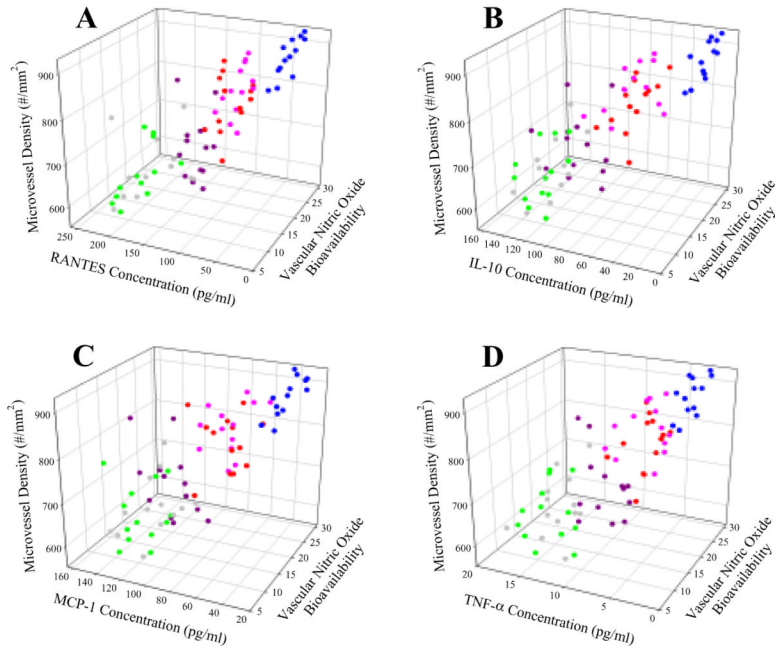

Figure 8.

Relationships between the four most significant markers of inflammation (identified using discriminant analyses; please see text for details), vascular NO bioavailability, and gastrocnemius muscle microvessel density for animals in the present study. Data are presented for RANTES (Panel A), IL-10 (Panel B), MCP-1 (Panel C), and TNF-α (Panel D), and the same color coding is used as in Figure 4; LZR (light blue), OZR (green), and OZR+GEM (grey), OZR+PRO (purple), OZR+SIM (orange) and OZR+ATOR (red).

NIH-PA Author Manuscript
NIH-PA Author Manuscript
NIH-PA Author Manuscript

Table 1

Characteristics of animal groups within the present study.

	Age	LZR	OZR	OZR-GEM	OZR-PRO	OZR-SIM	OZR-ATOR
Mass (g)	7w	155±5	241±6 *	254±8 *	250±9 *	247±8 *	245±5 *
	10w	238±6	401±8 *	398±7 *	400±9 *	405±8 *	408±7 *
	13w	304±7	513±10 *	520±10 *	508±12 *	506±9 *	501±8 *
	17w	369±5	628±12 *	630±12 *	625±13 *	622±12 *	618±9 *
MAP (mmHg)	7w	98±4	95±5	97±5	98±6	93±5	99±4
	10w	99±5	99±5	102±6	100±5	99±4	100±5
	13w	102±5	112±6	115±6	112±8	102±6	104±6
	17w	102±4	129±5 *	127±5 *	123±4 *	118±4 *	113±5 *†
Glucose (mg/dl)	7w	93±7	98±4	104±7	102±8	96±8	93±6
	10w	96±6	103±7	105±8	104±9	101±9	105±8
	13w	99±7	123±8 *	128±8 *	128±8 *	128±6 *	121±8 *
	17w	106±9	168±10 *	170±8 *	169±11 *	150±7 *	155±8 *
Insulin (ng/ml)	7w	1.0±0.3	3.2±0.5 *	4.1±0.6 *	3.6±0.7 *	2.9±0.5 *	3.0±0.6 *
	10w	1.1±0.2	4.9±0.7 *	5.4±0.6 *	6.0±0.6 *	4.8±0.6 *	4.3±0.5 *
	13w	1.2±0.3	7.9±0.6 *	7.5±0.7 *	7.8±0.8 *	6.0±0.6 *	5.7±0.6 *
	17w	1.2±0.2	9.0±0.8 *	8.2±0.6 *	9.1±0.9 *	6.4±0.8 *†	6.5±0.6 *†
Chol (mg/dl)	7w	80±7	98±8	95±10	95±9	91±9	94±6
	10w	82±6	106±7 *	84±8 †	83±9 †	83±8 †	84±7 †
	13w	77±8	128±10 *	87±9 †	88±9 †	85±9 †	85±9 †
	17w	71±10	142±12 *	86±9 †	84±11 †	82±11 †	81±12 †
TG (mg/dl)	7w	101±8	175±9 *	178±12 *	176±10 *	180±11 *	176±11 *
	10w	106±7	247±11 *	249±14 *	255±14 *	252±12 *	258±14 *
	13w	124±10	341±12 *	338±11 *	338±13 *	290±14 *†	302±13 *†
	17w	140±12	360±15 *	342±20 *	330±14 *†	320±15 *†	316±16 *†
N-tyrosine (ng/ml)	7w	9±2	16±4	17±4	12±4	13±4	14±3

Microcirculation. Author manuscript; available in PMC 2012 April 24.

Age	LZR	OZR	OZR-GEM	OZR-PRO	OZR-SIM	OZR-ATOR
10w	11±3	25±4*	26±4*	20±3*	16±4	15±5
13w	12±3	49±7*	45±7*	30±6*†	24±5*	25±4*†
17w	12±3	61±6*	53±5*	40±5*†	29±5*†	27±5*†

*p<0.05 vs. LZR

†p<0.05 vs. OZR.

NIH-PA Author Manuscript NIH-PA Author Manuscript NIH-PA Author Manuscript

NIH-PA Author Manuscript
NIH-PA Author Manuscript
NIH-PA Author Manuscript

Microcirculation. Author manuscript; available in PMC 2012 April 24.

Table 2

Plasma markers of inflammation (pg/ml) in the present study.

	Age	LZR	OZR	OZR-GEM	OZR-PRO	OZR-SIM	OZR-ATOR
IL-1β	7w	9.2±0.7	9.4±0.6	9.1±0.8	8.5±1.0	8.5±0.8	8.4±0.5
	10w	9.4±0.6	13.4±1.8 *	12.2±1.6 *	12.6±1.8 *	11.0±1 .4 *	10.8±1.1 *
	13w	9.8±0.7	18.5±2.0 *	18.3±1.9 *	16.8±1.7 *	12.0±1.9 *†	12.2±1.8 *†
	17w	10.2±0.8	23.2±2.5 *	19.8±2.2 *	18.5±2.0 *	14.4±1.8 †	15.0±2.0 †
IL-6	7w	26.2±4.8	35.5±5.1	33.8±4.6	29.8±5.3	28.0±4.5	31.1±4.4
	10w	30.8±5.4	40.5±5.4	36.2±6.0	34.3±5.5	29.9±4.3	35.0±5.1
	13w	36.8±5.6	68.6±6.1 *	65.2±5.6 *	64.6±5.8 *	38.4±6.1 †	40.6±4.6 †
	17w	38.6±4.6	79.8±5.7 *	77.2±6.6 *	71.0±6.4 *	52.4±5.8 †	53.9±6.1 †
IL-10	7w	14.6±2.6	24.8±4.0	22.0±4.1	16.5±3.8	15.2±3.8	14.6±3.1
	10w	15.2±3.6	80.3±6.7 *	75.3±8.0 *	64.4±9.0 *	51.0±6.8 *†	49.5±5.8 †
	13w	16.4±3.7	116.4±10.5 *	108.8±10.4 *	104.3±8.9 *	68.5±7.6 *†	62.4±6.8 *†
	17w	18.4±3.0	124±11.5 *	117.4±10.4 *	114.4±12.0 *	74.4±9.4 *†	68.8±11.2 *†
TNF-α	7w	2.0±0.4	5.0±1.0 *	5.1±0.9 *	4.6±0.7 *	3.9±0.7 *	3.5±0.6 *
	10w	2.5±0.4	8.9±1.0 *	8.4±1.1 *	7.2±1.2 *	5.8±0.8 *†	6.3±1.1 *†
	13w	3.2±0.3	10.3±1.6 *	9.8±0.9 *	8.6±1.8 *	5.0±1.2 †	5.7±1.6 †
	17w	3.4±0.4	10.4±1.4 *	10.8±1.2 *	8.8±1.5 *	6.2±1.4 †	6.8±1.6 †
RANTES	7w	28.0±4.7	34.2±4.8	35.0±5.1	33.4±4.9	31.3±5.5	29.6±4.6
	10w	32.2±4.6	66.6±7.9 *	60.4±8.2 *	53.4±5.3 *	43.4±5.8 †	44.2±4.7 †
	13w	36.4±4.8	120.2±10.3 *	117.4±9.9 *	108.8±10.9 *	85.4±9.9 *†	80.8±7.9 *†
	17w	40.1±5.3	187.2±14.1 *	176.8±15.8 *	138.4±14.8 *†	97.8±14.0 *†	102.8±13.6 *†
MCP-1	7w	36.6±5.8	45.0±5.9	43.8±5.2	45.6±4.9	40.4±5.1	41.2±6.0
	10w	36.8±4.7	57.7±10.5	54.9±12.0	51.5±6.4	43.6±5.2 *†	42.5±5.0 *
	13w	42.1±4.6	98.4±10.4 *	95.6±10.6 *	81.0±8.9 *	66.4±9.4 *†	62.2±6.3 *†
	17w	42.2±5.8	120.2±10.8 *	118.4±12.0 *	116.6±14.2 *	80.4±12.1 *†	77.8±11.4 *†
VEGF	7w	35.6±5.0	39.6±6.1	37.0±4.6	40.2±4.5	38.3±4.3	39.6±5.3

Age	LZR	OZR	OZR-GEM	OZR-PRO	OZR-SIM	OZR-ATOR
10w	41.1±5.3	55.5±4.5*	56.2±4.8*	50.2±5.3*	53.4±4.9*	55.5±4.5*
13w	39.2±5.3	62.9±6.7*	60.6±5.7*	58.6±6.1*	54.6±5.1*	56.9±6.4*
17w	38.9±4.1	68.7±5.4*	66.2±6.1*	61.8±5.8*	57.4±4.5*	58.8±4.8*

* $p<0.05$ vs. LZR

† $p<0.05$ vs. OZR.

NIH-PA Author Manuscript
NIH-PA Author Manuscript
NIH-PA Author Manuscript

NIH-PA Author Manuscript
NIH-PA Author Manuscript
NIH-PA Author Manuscript

Table 3

Structure matrix of results from discriminant analyses for markers of inflammation between animal groups in the present study.

Age	7 Weeks		10 Weeks		13 Weeks		17 Weeks	
Functions	**1**	**2**	**1**	**2**	**1**	**2**	**1**	**2**
% of Variance	81.7	12.0	96.2	2.6	97.3	3.0	98.3	1.5
Canonical Correlation	0.907	0.636	0.975	0.581	0.988	0.746	0.964	0.405
RANTES	---	---	0.364	0.683*	0.504	0.289	0.647*	−0.760*
IL-10	0.390	0.700*	0.531*	−0.182	0.576*	−0.389	0.521	0.593
MCP-1	0.368	−0.049	0.384	0.428	0.465	0.568*	0.501	0.452
TNF-α	0.553*	−0.568	0.401	−0.173	0.244	−0.300	---	---

* represents the largest absolute correlation between each variable and any discriminant function.

Microcirculation. Author manuscript; available in PMC 2012 April 24.